Eur J Nucl Med Mol Imaging (2011) 38:97–107
DOI 10.1007/s00259-010-1596-9

ORIGINAL ARTICLE

Development of a potent DOTA-conjugated bombesin antagonist for targeting GRPr-positive tumours

Rosalba Mansi · Xuejuan Wang · Flavio Forrer · Beatrice Waser · Renzo Cescato · Keith Graham · Sandra Borkowski · Jean Claude Reubi · Helmut R. Maecke

Received: 28 May 2010 / Accepted: 4 August 2010 / Published online: 18 August 2010

Abstract
Purpose Radiolabelled somatostatin-based antagonists show a higher uptake in tumour-bearing mouse models than agonists of similar or even distinctly higher receptor affinity. Very similar results were obtained with another family of G protein-coupled receptor ligands, the bombesin family. We describe a new conjugate, RM2, with the chelator DOTA coupled to D-Phe-Gln-Trp-Ala-Val-Gly-His-Sta-Leu-NH_2 via the cationic spacer 4-amino-1-carboxymethyl-piperidine for labelling with radiometals such as ^{111}In and ^{68}Ga.
Methods RM2 was synthesized on a solid support and evaluated in vitro in PC-3 cells. IC_{50} and K_d values were determined. The antagonist potency was evaluated by immunofluorescence-based internalization and Ca^{2+} mobilization assays. Biodistribution studies were performed in PC-3 and LNCaP tumour-bearing mice with ^{111}In-RM2 and ^{68}Ga-RM2, respectively. PET/CT studies were performed on PC-3 and LNCaP tumour-bearing nude mice with ^{68}Ga-RM2.
Results RM2 and ^{111}In-RM2 are high-affinity and selective ligands for the GRP receptor (7.7±3.3 nmol/l for RM2; 9.3±3.3 nmol/l for ^{nat}In-RM2). The potent antagonistic properties were confirmed by an immunofluorescence-based internalization and Ca^{2+} mobilization assays. ^{68}Ga- and ^{111}In-RM2 showed high and specific uptake in both the tumour and the pancreas. Uptake in the tumour remained high (15.2±4.8%IA/g at 1 h; 11.7±2.4%IA/g at 4 h), whereas a relatively fast washout from the pancreas and the other abdominal organs was observed. Uptake in the pancreas decreased rapidly from 22.6±4.7%IA/g at 1 h to 1.5±0.5% IA/g at 4 h.
Conclusion RM2 was shown to be a potent GRPr antagonist. Pharmacokinetics and imaging studies indicate that ^{111}In-RM2 and ^{68}Ga-RM2 are ideal candidates for clinical SPECT and PET studies.

Keywords Prostate cancer · Gastrin-releasing peptide receptor · Bombesin · Gallium-68 · Indium-111

R. Mansi · X. Wang · H. R. Maecke
Division of Radiological Chemistry, University Hospital Basel, Basel, Switzerland

F. Forrer
Institute of Nuclear Medicine, University Hospital Basel, Basel, Switzerland

B. Waser · R. Cescato · J. C. Reubi
Division of Cell Biology and Experimental Cancer Research, Institute of Pathology, University of Berne, Berne, Switzerland

K. Graham · S. Borkowski
Global Drug Discovery, Bayer Schering Pharma AG, Berlin, Germany

R. Mansi · H. R. Maecke (✉)
Department of Nuclear Medicine, University of Freiburg, Hugstetterstrasse 55, 79106 Freiburg, Germany
e-mail: helmut.maecke@uniklinik-freiburg.de

F. Forrer
Erasmus Medical Centre, Nuclear Medicine, Rotterdam, The Netherlands

Introduction

Radiolabelled peptides have attracted considerable interest because of their wide applicability in the development of target-specific radiopharmaceuticals [1, 2]. Somatostatin receptor targeting is an established method to image and treat somatostatin receptor-positive tumours [3]. Generally, the good internalization properties of agonists have been

considered crucial for an efficient accumulation of a radioligand in cells to give optimal tumour visualization in vivo [4, 5]. We have recently shown for somatostatin receptors 2 and 3, that antagonists have a higher tumour uptake than the corresponding agonists despite a very low internalization rate [6]. Among the different regulatory peptides explored for tumour targeting, bombesin and bombesin derivatives have attracted significant interest as they exhibit high affinity for the gastrin-releasing peptide receptor (GRPr), which is highly expressed on major human tumours such as prostate [7, 8], breast [9, 10] and gastrointestinal stromal tumours [11] and small-cell lung cancer (SCLC) [12]. Several radiolabelled bombesin analogues have been developed and their clinical and preclinical applications in targeting GRPr-positive tumours have been reported [13–16]. Bombesin elicits a broad spectrum of biological activities and may be involved as an autocrine growth factor in the pathophysiology of SCLC and other cancer types [17].

Due to the mitogenic properties of bombesin agonists, there has been considerable interest in the design of metabolically stable and selective GRPr antagonists and in the development of radiolabelled peptides for imaging (PET, SPECT) and targeted radionuclide therapy. Several classes of bombesin antagonists have been explored by the modification of the C-terminal residues of naturally amidated bombesin agonists [18, 19]. Cescato et al. [20] demonstrated the superiority of ^{99m}Tc-demobesin1 as a tumour-targeting agent with respect to a comparably potent radioagonist. Further, Abd-Elgaliel et al. [21] developed the ^{111}In-DOTA-amino-hexanoyl-[D-Phe^{6}, Leu-NHCH$_2$CH$_2$CH$_2$CH$_3$^{13}, des-Met^{14}]-BBN(6-14) conjugate, supporting the use of radiolabelled bombesin antagonists as potential candidates for in vivo imaging of GRPr-positive tumours. Very recently, we reported a direct comparison of a potent radiolabelled statin-based antagonist ^{111}In-RM1 and the potent agonist ^{111}In-AMBA [22]. Despite the lower GRPr affinity, the radioantagonist showed higher tumour uptake and superior pharmacokinetics than the radioagonist.

We describe here the synthesis and the pharmacological evaluation of a new DOTA-conjugated bombesin antagonist, RM2 (DOTA-4-amino-1-carboxymethyl-piperidine-D-Phe-Gln-Trp-Ala-Val-Gly-His-Sta-Leu-NH$_2$), supporting our hypothesis of the superiority of G protein-coupled receptor antagonists over agonists in vivo. We have shown earlier that positive charges at the N-terminal of bombesin-based agonists (BN(7-14)) lead to improved bombesin receptor affinities (Zhang H.; PhD thesis, University of Basel, 2006. http://edoc.unibas.ch/586). We were interested to determine if a similar effect could also be seen when employing antagonists. Therefore we linked DOTA (1,4,7,10-tetraazacyclododecane-1,4,7,10-tetraacetic acid) [23] via a positively charged spacer (4-amino-1-carboxymethyl-piperidine) to the potent antagonist JMV594 [24] and evaluated the use of the ^{111}In-labelled conjugate for SPECT and the ^{68}Ga-labelled peptide for PET. The antagonistic properties of the conjugate were evaluated in vitro using an immunofluorescence-based internalization assay and inhibition of Ca^{2+} mobilization assay using agonists. We were interested to determine if there is a difference between the use of an androgen-dependent and an androgen-independent tumour xenograft. Therefore its pharmacokinetics were studied in PC-3 and LNCaP tumour-bearing nude mice using SPECT/CT and PET/CT.

Materials and methods

Chemicals

All chemicals were obtained from commercial sources and used without additional purification. Rink amide 4-methyl-benzhydrylalanine (MBHA) resin and all the Fmoc-protected amino acids are commercially available from NovaBiochem (Laeufelfingen, Switzerland), DOTA (^{t}Bu)$_3$ from Chematec (Dijon, France), Fmoc-4-amino-1-carboxymethyl-piperidine from NeoMPS (Strasbourg, France) and ^{111}InCl$_3$ from Covidien Medical (Petten, The Netherlands). BIM26226 [25] was provided by Ipsen Biotech (Paris, France). Electrospray ionization mass spectroscopy (ESI-MS) was carried out with a Finnigan SSQ 7000 spectrometer (Bremen, Germany). Analytical high-performance liquid chromatography (RP-HPLC) was performed on a Hewlett Packard 1050 HPLC system with a multiwavelength detector and a flow-through Berthold LB 506 Cl γ-detector using a Macherey-Nagel Nucleosil 120 C$_{18}$ column (Oensingen, Switzerland) (eluent A comprising 0.1% TFA in water, eluent B comprising acetonitrile; gradient 0–30 min, 95% to 55% A; flow 0.750 ml/min). Semipreparative RP-HPLC was performed on a Metrohm HPLC system LC-CaDI 22-14 (Herisau, Switzerland) with a Macherey-Nagel VP 250/21 Nucleosil 100-5 C$_{18}$ column (eluent A comprising 0.1% TFA in water, eluent B comprising acetonitrile; gradient: 0–20 min, 95% to 30% A; flow 15 ml/min). Quantitative gamma counting was performed on a COBRA 5003 γ-system well counter from Packard Instruments.

Human embryonic kidney 293 (HEK293) cells, stably expressing the HA epitope-tagged human GRPr (HEK-GRPr), were generated as previously described [20] and cultured at 37°C in an atmosphere containing 5% CO_2 in DMEM with GlutaMAX-I containing 10% (v/v) fetal bovine serum (FBS), 100 U/ml penicillin, 100 μg/ml streptomycin and 750 μg/ml G418. Human prostate cancer cells (PC-3) were obtained from ATCC (Manassas, VA), cultured in DMEM or in Ham's F-12 K medium,

supplemented with vitamins, amino acids, penicillin/streptomycin and 10% FBS in a humidified atmosphere containing 5% CO_2 at 37°C. LNCaP cells were cultured in RPMI 1640 medium supplemented with 1n*M* of synthetic androgen R1881 (NEN), amino acids, penicillin/streptomycin, sodium pyruvate and 10% FBS in a humidified atmosphere containing 5% CO_2 at 37°C. All culture reagents were from Invitrogen (Basel, Switzerland) or from BioConcept (Allschwil, Switzerland).

Synthesis of peptide conjugate and metallation

The peptide–chelator conjugate RM2 was synthesized manually according to standard Fmoc chemistry [26] using Rink amide MBHA resin. The spacer and the prochelator DOTA(^{t}Bu)$_3$ were consecutively coupled to the peptide with HATU as activating agent. The peptide conjugate was purified according to the method of Heppeler et al. [23]. The peptide was purified by RP-HPLC and characterized by ESI-MS. The conjugate was complexed with $^{nat}InCl_3$ using a previously described procedure [14]. The pure product (yields ranging from 70% to 80%) after lyophilization was analysed by analytical RP-HPLC and characterized by ESI-MS.

Radiolabelling

^{111}In-RM2 was prepared by dissolving 10 μg of peptide in 250 μl of sodium acetate buffer (0.4 mol/l, pH 5.0) and incubating with $^{111}InCl_3$ (110–220 MBq) for 30 min at 95°C. To obtain structurally characterized homogeneous ligands, 1 equivalent of $^{nat}InCl_3 \cdot 5H_2O$ was added and the final solution incubated again at 95°C for 30 min. For biodistribution studies the labelling was performed following the same procedure but without the addition of the In^{3+} salt.

The $^{68}GaCl_3$ was provided by Charité CVZ Zentrales Radionuklid Labor (Berlin, Germany). HEPES solution (350 μl, 0.25 *M*) was added to an aqueous solution of RM2 (20 μL/20 μg) in a Wheaton vial. $^{68}GaCl_3$ solution (400 μl, 200–240 MBq; 97.6% acetone/ 0.05 *M* HCl) was added and the pH adjusted to 3.6–3.9. The solution was heated in a microwave at 75 W (95°C) for four times for 30 s each time and with 30 s between each heating. The reaction mixture was diluted with 5 ml of water and purified through a SepPak C18 cartridge preconditioned as described previously [27]. The product was eluted with EtOH (500 μl) and the radiochemical purity was checked by HPLC and instant thin-layer chromatography.

Receptor binding affinity and selectivity

IC_{50} values of RM2 and ^{nat}In-RM2 were determined by in vitro GRPr autoradiography on cryostat sections of well-characterized prostate carcinomas as described previously [7, 28]. The radioligand used was [^{125}I-Tyr^4]-bombesin, known to preferentially bind to the GRPr [29], and [^{125}I-D-Tyr^6, β-Ala^{11}, Phe^{13}, Nle^{14}]BN(6-14) as universal bombesin receptor ligand. The binding affinity profile for the three bombesin receptor subtypes was determined as described in detail previously [30].

The cellular binding saturation experiments were performed using increasing concentrations of the $^{111/nat}$In-DOTA peptide ranging from 0.1 to 1000 nmol/l. Confluent PC-3 cells were seeded into six-well plates (about 1.0×10^6 cells) 24 h before starting the experiments. For blocking experiments, 1 mmol/l of BIM26226 ([D-F$_5$Phe^6,Ala^{11}]BN(6-13) OMe) [25] was used. For each radioligand, triplicates were prepared for every concentration, for both total binding and nonspecific binding. Before adding the radioligands to the wells, the plates were placed on ice for 30 min. After adding the radioligands and BIM26226 for nonspecific binding, the plates were incubated for 2 h at 4°C. The binding buffer was then aspirated and the cells were washed twice with ice-cold phosphate-buffered saline (pH 7.4); this represented the free fraction. Finally, the cells were collected with 1 *N* NaOH; this corresponded to the bound fraction. Specific binding was calculated by subtracting nonspecific from total binding at each concentration of radioligand. Affinity (K_d) and binding site density (B_{max}) were calculated from Scatchard plots using Origin 7.5 software (Microcal Software, Northampton, MA).

Internalization

For internalization experiments, approximately 3 kBq of $^{111/nat}$In-labelled peptide (0.25 pmol) was added to the medium and the cells were incubated (in triplicate) for 0.5, 1, 2 and 4 h at 37°C in an atmosphere containing 5% CO_2. A large excess of BIM26226 was used (2 μmol/l, 100 μl) to determine nonspecific internalization. At each time point the cells were treated as recently described [14].

Immunofluorescence microscopy

Immunofluorescence microscopy-based internalization assays with HEK-GRPr cells were performed as previously described [20]. HEK-GRPr cells were treated with either 10 nmol/l bombesin or 1 μmol/l RM2 or, to evaluate potential antagonism, with 10 nmol/l bombesin in the presence of a 100-fold excess of RM2 for 30 min at 37°C in an atmosphere containing 5% CO_2 in growth medium, and then processed for immunofluorescence microscopy using first mouse monoclonal HA-epitope antibody (Covance, Berkeley, CA) at a dilution of 1:1000 and second Alexa Fluor 488 goat anti-mouse IgG (H + L, Molecular Probes, Eugene, OR) at a dilution of 1:600. The cells were imaged

using a Leica DM RB immunofluorescence microscope and an Olympus DP10 camera.

Ca^{2+} mobilization assay

Intracellular Ca^{2+} mobilization was measured in PC-3 cells using a Fluo-4NW calcium assay kit (Molecular Probes, Eugene, OR) as described previously [20]. In brief, PC-3 cells were seeded (10,000 cells per well) into 96-well plates and cultured for 2 days at 37°C in an atmosphere containing 5% CO_2. On the day of the experiment, the cells were washed with assay buffer (1 × HBSS, 20 mmol/l HEPES) containing 2.5 mmol/l probenecid. The cells were then incubated with 100 μl/well Fluo-4NW dye in assay buffer for 30 min at 37°C in an atmosphere containing 5% CO_2 and then for a further 30 min at room temperature. The dye-loaded cells were transferred to a SpectraMax M2^e (Molecular Devices, Sunnyvale, CA) and intracellular Ca^{2+} mobilization was recorded in a kinetic experiment for 60 s at room temperature monitoring fluorescence emission at 520 nm (λ_{ex}=485 nm) in the presence of the compounds to be tested. Data are shown as percentage of the maximum calcium response obtained with ionomycin as reported previously [20].

Biodistribution experiments

All animal experiments were performed in compliance with the Swiss (no. 798) and German regulations for animal treatment.

The pharmacokinetics of ^{111}In-RM2 were evaluated in female nude mice (3 weeks old), implanted subcutaneously with 10 million PC-3 tumour cells, freshly expanded in a sterilized solution of phosphate-buffered saline (pH 7.4). The mice (20–22 g) were injected into the tail vein 11 days after inoculation with 10 pmol of radiolabelled peptides (about 0.18 MBq, 100 μl). For the determination of nonspecific uptake in tumour or receptor-positive organs, a group of four animals were preinjected (5 min) with 0.02 μmol of unlabelled peptide. At 1, 4, 24, 48 and 72 h the mice (in groups of 4 to 11) were killed and organs of interest were collected, rinsed, blotted, weighed and counted in a γ-counter. The percentage of injected activity per gram (%IA/g) was calculated for each tissue.

The biodistribution experiments with ^{68}Ga-RM2 were performed using male nude mice (NMRI nu/nu, Taconic) at 3–4 weeks of age. The animals were implanted subcutaneously with PC-3 (2×10^6 cells/mouse) or LNCaP cells (1×10^7 cells/mouse) in the right shoulder. Mice to be injected with LNCaP cells were pretreated with testosterone pellets (12.5 mg, 90 days release; IRA, Sarasota, FL) implanted 3–4 days before tumour cell inoculation. For the tumour cell implantation, cells were suspended in Matrigel (BD Biosciences) to a final volume of 100 μl. The animals (30–35 g) were injected intravenously 4 weeks after implantation with 80 pmol of ^{68}Ga-RM2 (100 μl, 150–240 kBq). The animals were killed at different times from 20 to 120 min after injection (three mice for each time point). In addition, a group of three mice were preinjected with 0.06 μmol of RM2 and killed at 1 h later to determine nonspecific uptake.

Imaging

SPECT/CT was performed with a four-head multiplexing multipinhole camera (NanoSPECT/CT; Bioscan). Each head was equipped with a tungsten-based collimator of nine 1.4-mm diameter pinholes. The apertures used in this study provided a reconstructed resolution in the submillimetre range at 140 keV [31]. Two PC-3 tumour-bearing nude mice were anaesthetized with 4% isoflurane/oxygen 24 h after intravenous injection of 42 MBq of ^{111}In-RM2. The acquisition mode was helical for both modalities and the time per view for the SPECT scans was 30 s. The acquisition time was approximately 15 min for the SPECT scan. CT scans were performed with an integrated CT scanner using a tube voltage of 45 kV and an exposure time of 1,500 ms per view. After acquisition, the SPECT data were reconstructed iteratively with HiSPECT software (Scivis). The CT data were reconstructed using a cone-beam filtered back-projection. The SPECT and CT data were automatically coregistered as both modalities shared the same axis of rotation. The fused datasets were analysed in InVivoScope postprocessing software (Bioscan).

The PET/CT studies were performed using a multimodality Inveon PET/CT camera (Siemens). Approximately 50 min after intravenous injection of about 7 MBq ^{68}Ga-RM2 (400 pmol) PC-3 and LNCaP tumour-bearing mice were anaesthetized with 4% isoflurane/oxygen. At a constant low breathing frequency (about 60 min^{-1}) animals were transferred to the camera bed and fixed for static PET imaging with a duration of 30 min followed by CT. Breathing frequency and body temperature of the animals were continuously monitored. Images were recorded, reconstructed and analysed using Inveon-specific acquisition and research software packages.

Results

RM2 (Fig. 1) was synthesized using solid-phase peptide synthesis (Fmoc chemistry). The ^{111}In-RM2 conjugate was obtained in >95% radiolabelling yield at a maximum specific activity of 30 GBq/μmol. ^{68}Ga-RM2 was obtained with a specific activity of 10 GBq/μmol. The metallated and unmetallated conjugates were purified by RP-HPLC and characterized by ESI-MS (RM2, 1678.1 [M + K^+]; ^{nat}In-RM2, 1755.7 [M + H^+]).

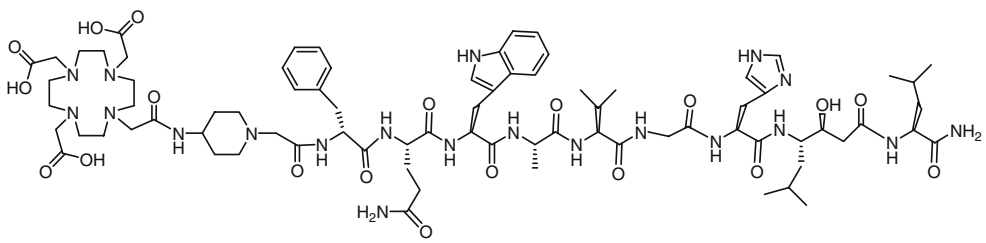

Fig. 1 Structure of unlabelled peptide chelator conjugate RM2

Figure 2a shows the cellular uptake of ^{111}In-RM2 in PC-3 cells. The amount of surface associated activity exceeded the amount of internalized activity at all time points. At 4 h the amount of specifically internalized activity was 3.7±0.4% while 15.9±0.9% was surface-bound. GRPr affinities of RM2 and ^{nat}In-RM2 were determined by a competitive binding assay using [^{125}I-Tyr^4]BN as radioligand (Table 1). On the human GRPr, the IC_{50} values were 7.7±3.3 nmol/l for RM2 and 9.3±3.3 nmol/l for ^{nat}In-RM2. The bombesin receptor subtype binding profile demonstrated excellent selectivity of RM2 in showing good binding affinity to GRPr (9.3±0.7 nmol/l) and >10^3 nmol/l to NMBr and BB3r. Saturation binding experiments were performed at 4°C by incubating for 2 h with increasing concentrations of $^{111/nat}$In-RM2 (Fig. 2b). The K_d value was 2.9±0.4 nmol/l while the B_{max} value was 1.1±0.05 nmol/l. This B_{max} value corresponding to 5.5×10^5 binding sites per cell is in agreement with literature data [32].

The antagonistic properties of RM2 were confirmed by a immunofluorescence-based internalization assay using HEK-GRPr cells. Figure 3 shows that 10 nmol/l bombesin was able to trigger receptor internalization into HEK-GRPr cells. RM2 was not able to stimulate GRPr internalization even at a concentration of 1,000 nmol/l. However, at a concentration of 1,000 nmol/l together with 10 nmol/l of bombesin, the peptide was able to prevent the bombesin-induced receptor internalization. The Ca^{2+} mobilization assay was performed to determine dose-response curves of the bombesin antagonist in PC-3 cells. RM2 behaved as an antagonist shifting the dose-response curve of bombesin to a higher molar range when present at a concentration of 10 μmol/l together with bombesin. Moreover, tested alone at 1 μmol/l and 10 μmol/l the peptide had no effect on intracellular calcium mobilization (Fig. 4).

Biodistribution data from PC-3 tumour-bearing athymic nude mice are shown in Table 2. ^{111}In-RM2 displayed fast blood clearance with 0.05±0.04 %IA/g remaining in the blood at 4 h after injection. The uptake in the organs of the gastrointestinal tract, which are known to express GRPr, such as the pancreas, stomach and intestine, was high and specific, but the radiopeptide was washed out quickly. The pancreas uptake decreased rapidly from 22.6±4.7%IA/g at 1 h to 1.5±0.5%IA/g at 4 h. High uptake was observed in the PC-3 tumour with 15.2±4.8%IA/g at 1 h and the uptake was still high at 4 h with 11.7±2.4%IA/g, and even at later time points (6.8±1.0 %IA/g at 24 h; 4.7±0.4%IA/g at 48 h; 4.1±0.3%IA/g at 72 h). The long retention in the tumour indicates that RM2 labelled with ^{177}Lu or ^{90}Y may be a successful therapeutic agent.

The radiopeptide was quickly washed out from nontarget tissues leading to very high tumour to normal organ ratios which increased over time. For instance, tumour to kidney

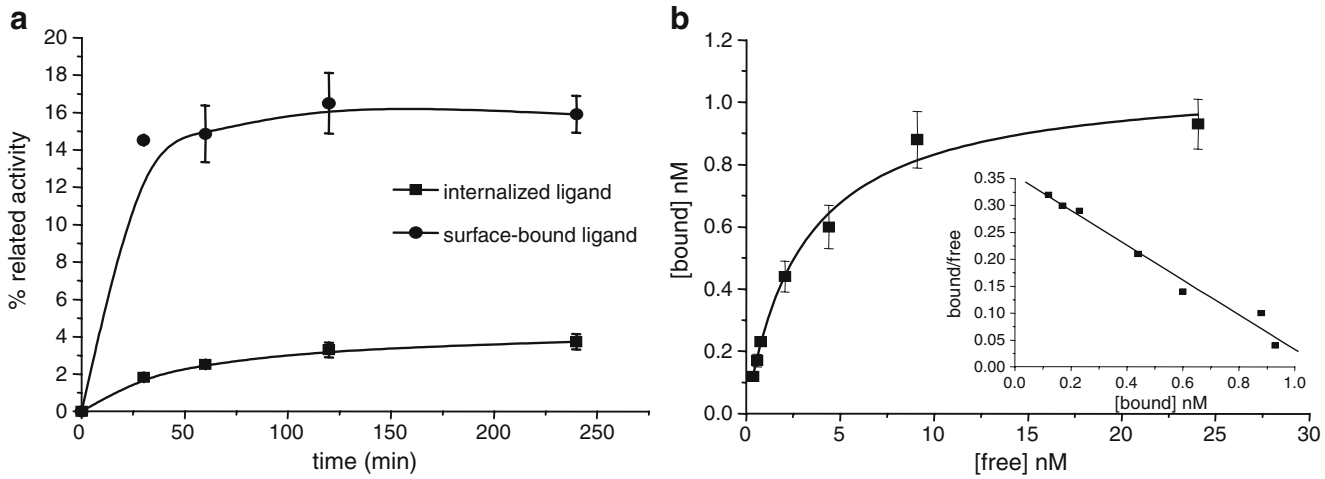

Fig. 2 **a** Internalization (*squares*) of ^{111}In-RM2 in PC-3 cells is low, while a higher percentage of the radioconjugate remains bound to cells (*circles*). Data are the mean values from three independent experiments performed in triplicate. **b** Scatchard plots of ^{111}In-RM2 from saturation-binding experiments on PC-3 cells. The graphs were produced using Origin 7.5 software (Microcal Software, Northampton, MA)

Table 1 Comparison of the K_d and IC_{50} values of RM1 and RM2 and their ^{nat}In-metallated counterparts

	RM1	^{nat}In-RM1	RM2	^{nat}In-RM2
IC_{50} (n*M*)	35±13	14±3.4	7.7±3.3	9.3±3.3
K_d (n*M*)		8.5±2.7		2.9±0.4

and tumour to blood ratios increased from 3.2 and 19.8 at 1 h to 5.5 and 6,840 at 24 h, respectively. SPECT/CT images of a PC-3 tumour-bearing mouse 24 h after injection of 42 MBq ^{111}In-RM2 illustrating the high uptake in the tumour are shown in Fig. 5.

Uptake in the GRPr rich tissues, as well as in the tumour, were found to be significantly reduced in the animals preinjected with an excess of cold peptide, indicating a specific GRPr-mediated uptake. The pharmacokinetics of ^{68}Ga-RM2 was studied in male nude mice bearing the androgen-independent PC-3 xenograft reported to show high GRPr expression (Table 3) or the androgen-dependent LNCaP xenograft that shows about 40-fold lower GRPr expression (Table 4) [33]. In PC-3 tumour-bearing mice

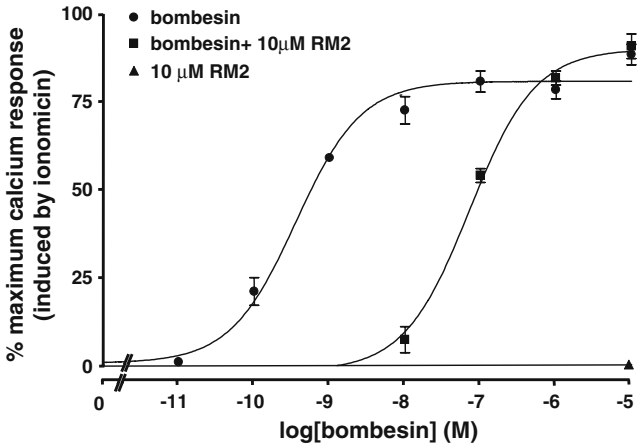

Fig. 4 Dose-response curves of the bombesin analogue RM2 determined by the Ca^{2+} mobilization assay. PC-3 cells were treated either with bombesin at concentrations ranging between 0.01 n*M* and 10 μ*M* alone (*circles*), or with bombesin at the same concentrations together with 10 μ*M* of the bombesin analogue RM2 (*squares*). RM2 behaves as an antagonist shifting the dose-response curve of bombesin to a higher molar range. When tested alone, RM2 at a concentration of 10 μ*M* (*triangles*) has no effect on calcium mobilization in PC-3 cells

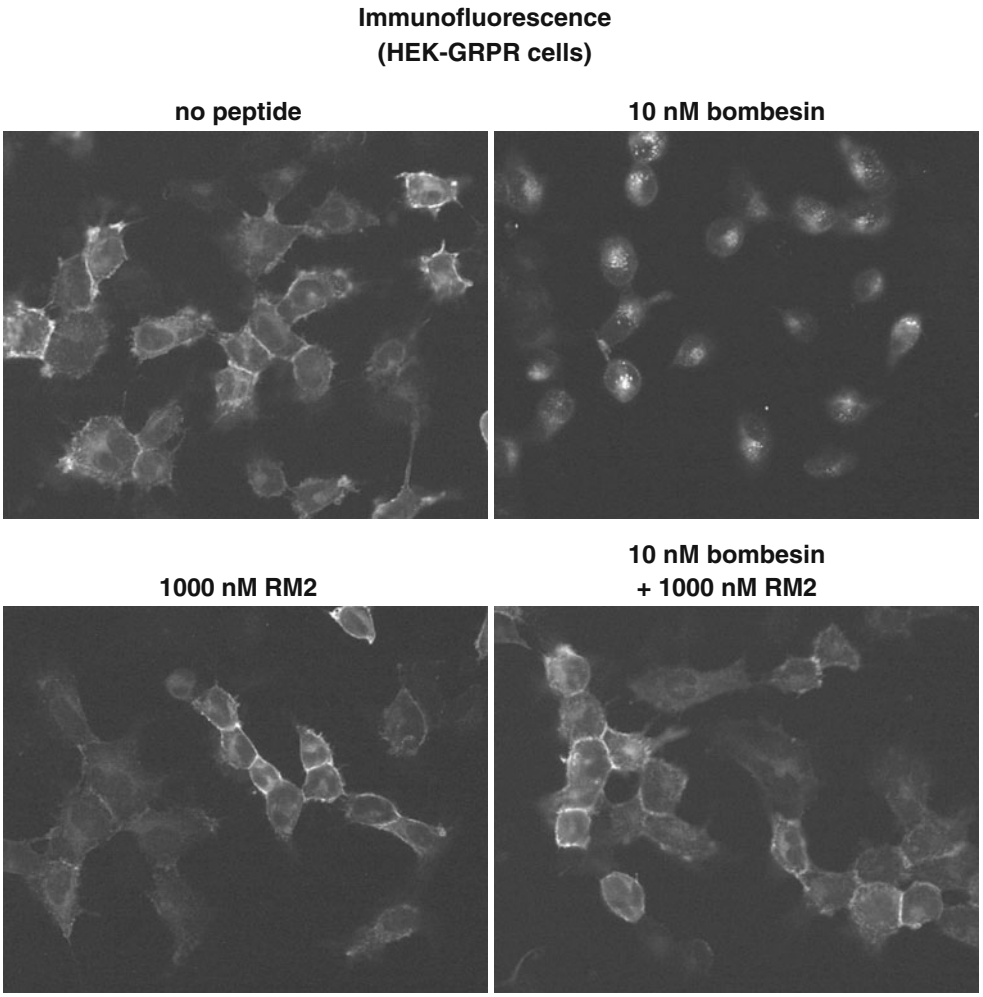

Fig. 3 GRP receptor internalization induced by bombesin is efficiently antagonized by the bombesin analogue RM2. *Top panels*: HEK-GRPr cells were treated for 30 min with vehicle (no peptide) or with 10 n*M* bombesin, a concentration inducing a submaximal internalization effect. *Bottom panels*: HEK-GRPr cells were treated for 30 min with 1000 n*M* RM2 alone or with 10 n*M* bombesin in the presence of 1000 n*M* RM2

Table 2 Biodistribution of ^{111}In-RM2 in female nude mice bearing PC-3 tumours. Values are means±SD %IA/g (n=4)

Organ	1 h	4 h	4 h blocking[a]	24 h	48 h	72 h
Blood	0.77±0.28	0.05±0.04	0.13±0.02	0.003±0.00	0.002±0.00	0.001±0.00
Heart	0.32±0.09	0.04±0.03	0.09±0.01	0.02±0.01	0.01±0.00	0.02±0.02
Liver	0.49±0.12	0.18±0.06	0.34±0.03	0.09±0.01	0.07±0.01	0.06±0.02
Spleen	0.53±0.20	0.12±0.06	0.16±0.02	0.06±0.02	0.05±0.01	0.06±0.03
Lung	0.70±0.30	0.10±0.07	0.19±0.01	0.04±0.03	0.11±0.24	0.04±0.02
Kidney	4.78±1.11	2.14±0.73	2.98±0.20	1.25±0.16	0.91±0.09	0.74±0.18
Stomach	3.15±0.78	1.07±0.15	0.12±0.02	0.06±0.02	0.03±0.01	0.05±0.01
Intestine	2.11±0.47	0.25±0.15	0.11±0.01	0.04±0.01	0.03±0.01	0.03±0.01
Adrenal	3.46±2.07	1.17±0.54	1.10±0.60	0.71±0.29	0.54±0.29	0.50±0.34
Pancreas	22.64±4.71	1.55±0.48	0.10±0.00	0.32±0.09	0.19±0.04	0.19±0.02
Pituitary	7.00±5.68	0.59±0.55	0.58±0.49	0.07±0.33	0.21±0.33	0.51±0.24
Muscle	0.29±0.17	0.05±0.04	0.06±0.02	0.02±0.01	0.01±0.01	0.02±0.01
Bone	0.91±0.68	0.35±0.57	0.35±0.11	0.20±0.18	0.12±0.11	0.15±0.05
Tumour	15.23±4.78	11.75±2.43	0.45±0.04	6.84±1.02	4.67±0.39	4.07±0.34
Tumour/blood ratio	19.8	235		2,280	2,335	4,070
Tumour/kidney ratio	3.2	5.5		5.5	5.1	5.5
Tumour/liver ratio	31.0	65.3		76.0	66.7	67.8
Tumour/muscle ratio	52.5	235		342	467	203

[a] Blocked with 20 nmol of RM2

high accumulation was found in the tumour (9.6±1.4%IA/g at 20 min). The uptake in the tumour increased with time reaching a maximum value of 14.7±2.1%IA/g at 80 min, while decreasing in the GRPr-positive organs (45.9±4.7% IA/g at 20 min and 22.4±6.6%IA/g at 80 min in the pancreas). The kidney uptake was comparable to the tumour uptake at 20 min, but decreased significantly; at 80 min the tumour to kidney ratio was 6. Most likely due to their lower GRPr expression status [34], LNCaP tumours showed lower uptake at each time point resulting in decreased tumour to target tissue ratios. The ^{68}Ga-RM2 was quickly cleared from the nontarget tissue and the blood. These pharmacokinetic data are reflected in the microPET/CT images presented in Fig. 6. Maximum intensity projections in PC-3 and LNCaP mice (unblocked and blocked with 100 μg RM2 per mouse) show the

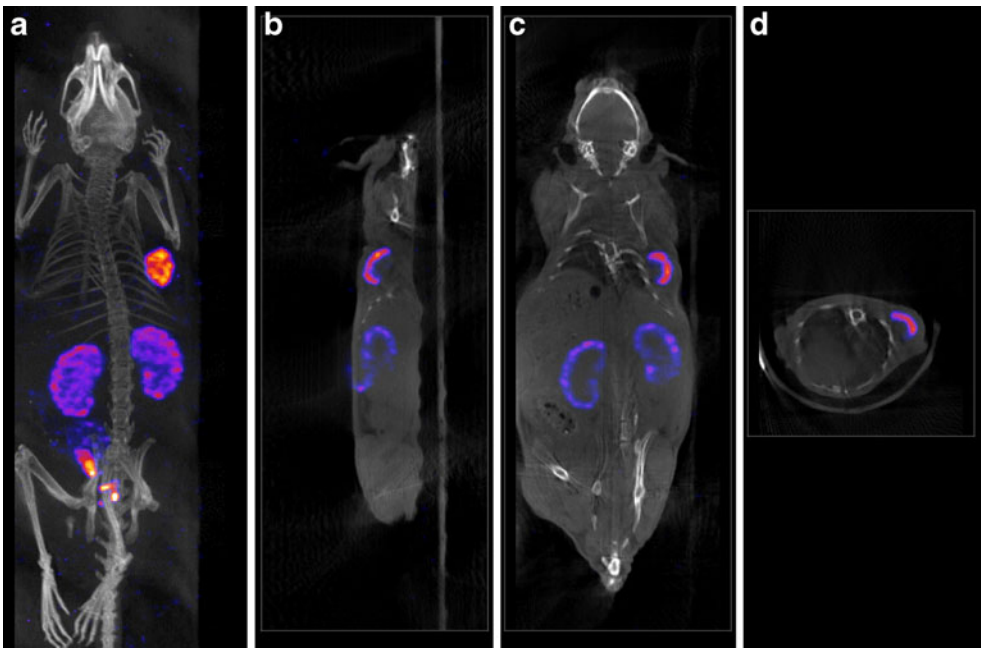

Fig. 5 SPECT/CT of a PC-3 tumour-bearing nude mouse 24 h after injection of 42 MBq ^{111}In-RM2. High specific uptake is seen in the xenografted tumour in the left shoulder. Significantly less activity is seen in the kidneys. Activity can also be seen in the bowel and the bladder. **a** Maximum intensity projection SPECT/CT image; **b–d** reconstructed slices through the xenografted tumour (**b**: sagittal, **c**: coronal, **d**: axial)

Table 3 Biodistribution of ^{68}Ga-RM2 in male nude mice bearing PC-3 tumours. Values are means ±SD %IA/g (n=4; urine values are %IA)

Organ	20min	60min	80min	100min	120min
Blood	1.67±0.51	0.59±0.12	0.51±0.15	0.46±0.09	0.32±0.06
Heart	0.67±0.22	0.27±0.09	0.22±0.09	0.27±0.07	0.20±0.05
Liver	0.87±0.19	0.39±0.03	0.47±0.04	0.30±0.10	0.29±0.07
Spleen	0.99±0.53	0.34±0.05	0.25±0.01	0.17±0.10	0.32±0.09
Lung	1.49±0.07	0.61±0.08	0.59±0.08	0.64±0.33	0.37±0.05
Kidney	9.71±4.66	3.34±0.54	2.41±0.42	1.90±0.38	2.23±0.02
Stomach	3.25±0.31	3.56±0.42	4.21±2.28	2.97±0.65	2.40±0.32
Intestine	2.87±0.81	2.67±1.14	3.77±2.76	1.73±0.10	3.28±1.78
Adrenal	8.46±0.94	1.10±0.60	2.30±1.49	3.76±2.53	2.36±0.26
Pancreas	46.95±4.71	30.74±1.97	22.43±6.65	19.40±0.47	16.00±1.85
Muscle	0.57±0.33	0.12±0.03	0.19±0.13	0.08±0.03	0.14±0.08
Bone	0.62±0.20	0.32±0.08	0.22±0.17	0.33±0.05	0.26±0.06
Tumour	9.59±1.45	14.11±1.88	14.66±2.12	11.33±3.87	13.61±0.64
Urine	36.89±6.62	68.50±6.69	75.16±11.38	75.94±4.93	81.46±10.97
Tumour/blood ratio	5.7	18.1	28.7	24.6	42.5
Tumour/kidney ratio	0.98	4.22	6.1	5.9	6.1
Tumour/liver ratio	11.0	36.2	31.2	37.8	46.9
Tumour/muscle ratio	16.8	117.6	77.1	141.6	97.2

specific tumour targeting and very low background. Predominant renal excretion was demonstrated by high kidney uptake and urinary bladder accumulation in conjunction with low uptake in the small bowel. Biodistribution and PET imaging indicated the excellent GRPr targeting mechanism of radiolabelled RM2 independent of the androgen responsiveness of the prostate cancer xenograft model used.

Discussion

The use of radiolabelled peptide antagonists for receptor targeting of tumours in vivo has attracted attention since the seminal paper of Ginj et al. [6]. It was shown that compared with agonists, somatostatin receptor antagonists are superior in terms of targeting more receptor binding sites and consequently demonstrate higher tumour uptake. Based on

Table 4 Biodistribution of ^{68}Ga-RM2 in male nude mice bearing LNCaP tumours. Values are means ±SD %IA/g (n=3; urine values are %IA)

Organ	20min	60min	80min	100min	120min
Blood	1.73±0.27	0.78±0.19	0.67±0.31	0.45±0.18	0.35±0.08
Heart	0.79±0.14	0.30±0.04	0.26±0.09	0.20±0.03	0.18±0.02
Liver	1.07±0.41	0.60±0.09	0.42±0.11	0.38±0.04	0.34±0.09
Spleen	1.22±0.63	0.49±0.24	0.29±0.06	0.41±0.18	0.33±0.15
Lung	1.57±0.29	0.61±0.01	0.61±0.16	0.49±0.17	0.33±0.07
Kidney	5.68±2.12	2.14±0.07	1.99±0.38	2.02±0.72	1.86±0.53
Stomach	4.23±0.53	3.94±1.12	3.52±0.91	2.58±0.79	4.10±2.66
Intestine	3.90±0.41	2.06±1.14	2.44±0.59	2.21±0.59	2.34±0.38
Adrenal	7.09±1.02	3.19±1.13	5.21±2.67	4.64±1.41	2.99±0.34
Pancreas	60.13±5.26	39.32±4.17	43.85±6.24	29.62±4.33	28.08±3.24
Muscle	0.40±0.04	0.22±0.06	0.17±0.05	0.13±0.02	0.12±0.03
Bone	0.55±0.14	0.29±0.12	0.21±0.06	0.24±0.05	0.19±0.05
Tumour	5.94±1.80	5.50±0.39	6.79±1.35	6.03±1.14	8.18±1.89
Urine	39.85±9.45	61.60±8.54	77.56±14.29	69.82±9.8	81.67±5.51
Tumour/blood	3.4	7.1	10.1	13.4	23.4
Tumour/kidney	1.0	2.6	3.4	3.0	4.4
Tumour/liver	5.5	9.2	16.2	15.9	24.0
Tumour/muscle	14.8	25	39.9	46.4	68.2

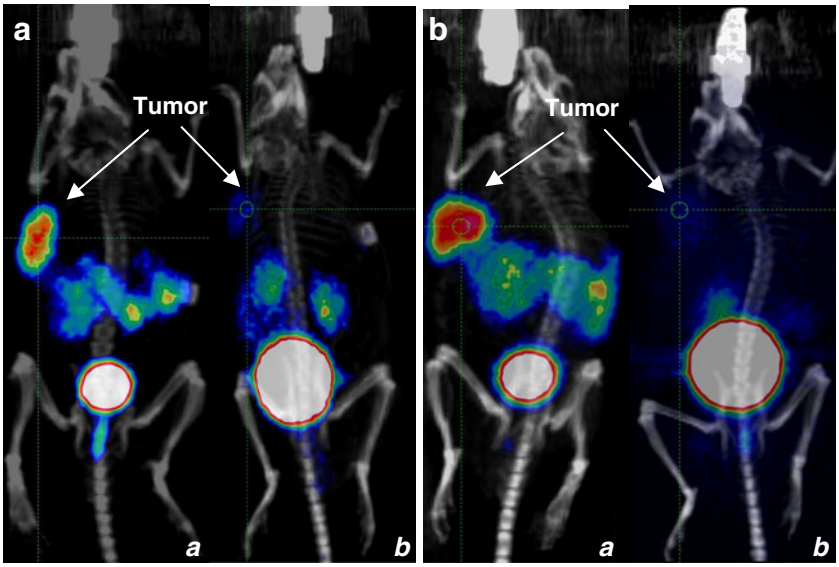

Fig. 6 MicroPET/CT images of LNCaP (**a**) and PC-3 (**b**) tumour-bearing nude mice after injection of ^{68}Ga-RM2 at 1 h (*a*) and 1 h blocking (*b*)

these results research groups have focused their attention on the development of new radioantagonists for tumour targeting [20, 21, 35]. Despite this progress little is known about structural parameters determining the antagonistic potential of radiometal-labelled bombesin-based antagonists, such as the influence of the metal complex, the spacer separating the reporting unit from the pharmacophoric peptide, receptor subtype profile etc. In addition, the origin of the long residence time in tumours found by us and others [20, 22] is not yet known.

We report here on the development of a DOTA-conjugated radiopeptide for the diagnosis and therapy of bombesin receptor-positive tumours. The DOTA monoamide coupled chelator can form complexes with a variety of trivalent and divalent radiometals to produce radiolabelled bioconjugates with high in vitro and in vivo stability [23]. In our previous work, the statin-based bombesin antagonist was linked via Gly-aminobenzoic acid to DOTA for a direct comparison with the potent agonist AMBA [22]. In order to potentially improve the pharmacological performance, a statin analogue was coupled to the positively charged spacer 4-amino-1-carboxymethyl piperidine. The K_d and the IC_{50} values of ^{nat}In-RM2 are indeed 3-fold and 1.5-fold higher, respectively, than those of RM1 [22], indicating that positive charges may be a structural motif to increase binding affinity (Table 1). Excellent antagonist properties of RM2 were confirmed by immunofluorescence and Ca^{2+} mobilization assays. The presence of a low concentration of RM2 inhibits the receptor internalization triggered by bombesin. In addition, the mobilization of Ca^{2+} caused by agonists was efficiently inhibited by RM2.

The pharmacokinetics of ^{111}In-RM2 were studied in PC-3 tumour-bearing nude mice. The radioconjugate was taken up by the tumour and the receptor-positive organs at early time points but it was washed out at a different rate; the pancreas uptake decreased by a factor of 14.6 within 4 h while the tumour uptake decreased by a factor of only 1.3 over the same time period. The uptake was specific and receptor-mediated; more than 95% of the uptake in the tumour and in the pancreas was blocked by preinjection of 20 nmol RM2. The fast clearance from the abdominal organs, including the pancreas, is consistent with the few reported data of bombesin-based radioantagonists [20–22] and it differs distinctly from the in vivo behaviour of the agonists that show high and persistent uptake in the abdominal organs [14–16, 36]. The reason for the different pharmacokinetic behaviour is not understood yet. It may be due to species differences (PC-3 is of human origin), or may result from a more efficient perfusion in the pancreas and intestine. The slow washout of ^{111}In-RM2 from the tumour is in contrast to that of ^{111}In-bomproamide [21] which showed as much as 70% loss within 4 h of injection. ^{111}In-Bomproamide also shows faster washout from the abdominal organs leading to similar tumour to background ratios. Despite the fact that ^{111}In-RM2 has an additional positive charge and threefold greater K_d value than our previously reported radioantagonist [22], we found little improvement in regard to overall pharmacokinetics except for a lower liver uptake leading to a significantly higher tumour to liver ratio.

The excellent tumour to kidney and tumour to background ratios led us to study this analogue as a PET imaging tool. We tested it in two animal models and with two different cell lines. The peptide was labelled with ^{68}Ga and studied in PC-3 and LNCaP tumour-bearing male nude mice. The PC-3 cell line is more representative of androgen-independent tumour cells while the LNCaP cell line is, currently, the closest representation of a human prostatic carcinoma in cell culture [37, 38]. The pharmaco-

kinetics of ^{68}Ga-RM2 in PC-3 tumours reflect what we observed with ^{111}In-RM2. Uptake in the tumour, in the target tissues and in the kidney was high at early time points but it decreased rapidly in all organs except the tumour. The biodistribution data of the LNCaP tumour-bearing nude mice showed similar pharmacokinetics but with lower tumour uptake. The lower tumour uptake is in line with the significant difference in the number of binding sites of the two cell lines [34]. In all cases the high tumour uptake and the high tumour to kidney ratio of ^{68}Ga-RM2 are well visualized in the PET/CT images of the PC-3 and LNCaP tumour-bearing nude mice. The ability of this conjugate, and more generally, of many antagonists already studied, to reach and maintain high tumour accumulation despite the low internalization may be due to strong receptor–antagonist interactions that produce a stable complex [39].

$^{111/nat}$In-RM2 behaved as an antagonist in several types of in vitro internalization experiments, showing a very poor receptor-mediated internalization in contrast to high surface binding. It prevented bombesin-induced receptor internalization in the immunofluorescence-based internalization experiment. The high and specific tumour uptake and the good tumour to background ratio at each time point indicate that this analogue is a good candidate for diagnostic purposes (PET/CT, SPECT/CT) and is potentially a good candidate for human studies.

Acknowledgments We thank Prof. Marion de Jong and Dr. Cristina Müller for support with the SPECT/CT measurements, Novartis Pharma for analytical assistance, M.L. Tamma and S. Tschumi for their expert technical help, and Bayer Schering Pharma for financial support.

Conflict of interest Rosalba Mansi, Xuejuan Wang, Flavio Forrer, Beatrice Waser, Renzo Cescato, Jean Claude Reubi and Helmut R. Maecke declare that they have no conflict of interest.

References

1. Reubi JC, Macke HR, Krenning EP. Candidates for peptide receptor radiotherapy today and in the future. J Nucl Med 2005;46 Suppl 1:67S–75S.
2. Heppeler A, Froidevaux S, Eberle AN, Maecke HR. Receptor targeting for tumor localisation and therapy with radiopeptides. Curr Med Chem 2000;7:971–94.
3. Eisenwiener K-P, Prata MIM, Buschmann I, Zhang H-W, Santos AC, Wenger S, et al. NODAGATOC, a new chelator-coupled somatostatin analogue labeled with [$^{67/68}$Ga] and [^{111}In] for SPECT, PET, and targeted therapeutic applications of somatostatin receptor (hsst2) expressing tumors. Bioconjug Chem 2002;13:530–41.
4. Bodei L, Paganelli G, Mariani G. Receptor radionuclide therapy of tumors: a road from basic research to clinical applications. J Nucl Med 2006;47:375–7.
5. Waser B, Tamma ML, Cescato R, Maecke HR, Reubi JC. Highly efficient in vivo agonist-induced internalization of sst2 receptors in somatostatin target tissues. J Nucl Med 2009;50:936–41.
6. Ginj M, Zhang H, Waser B, Cescato R, Wild D, Wang X, et al. Radiolabeled somatostatin receptor antagonists are preferable to agonists for in vivo peptide receptor targeting of tumors. Proc Natl Acad Sci U S A 2006;103:16436–41.
7. Markwalder R, Reubi JC. Gastrin-releasing peptide receptors in the human prostate: relation to neoplastic transformation. Cancer Res 1999;59:1152–9.
8. Sun B, Halmos G, Schally AV, Wang X, Martinez M. Presence of receptors for bombesin/gastrin-releasing peptide and mRNA for three receptor subtypes in human prostate cancers. Prostate 2000;42:295–303.
9. Gugger M, Reubi JC. Gastrin-releasing peptide receptors in non-neoplastic and neoplastic human breast. Am J Pathol 1999;155:2067–76.
10. Halmos G, Wittliff JL, Schally AV. Characterization of bombesin/gastrin-releasing peptide receptors in human breast cancer and their relationship to steroid receptor expression. Cancer Res 1995;55:280–7.
11. Reubi JC, Korner M, Waser B, Mazzucchelli L, Guillou L. High expression of peptide receptors as a novel target in gastrointestinal stromal tumours. Eur J Nucl Med Mol Imaging 2004;31:803–10.
12. Toi-Scott M, Jones CL, Kane MA. Clinical correlates of bombesin-like peptide receptor subtype expression in human lung cancer cells. Lung Cancer 1996;15:341–54.
13. Van de Wiele C, Dumont F, Vanden Broecke R, Oosterlinck W, Cocquyt V, Serreyn R, et al. Technetium-99m RP527, a GRP analogue for visualisation of GRP receptor-expressing malignancies: a feasibility study. Eur J Nucl Med 2000;27:1694–9.
14. Zhang H, Chen J, Waldherr C, Hinni K, Waser B, Reubi JC, et al. Synthesis and evaluation of bombesin derivatives on the basis of pan-bombesin peptides labeled with indium-111, lutetium-177, and yttrium-90 for targeting bombesin receptor-expressing tumors. Cancer Res 2004;64:6707–15.
15. Lantry LE, Cappelletti E, Maddalena ME, Fox JS, Feng W, Chen J, et al. ^{177}Lu-AMBA: Synthesis and characterization of a selective ^{177}Lu-labeled GRP-R agonist for systemic radiotherapy of prostate cancer. J Nucl Med 2006;47:1144–52.
16. Nock BA, Nikolopoulou A, Galanis A, Cordopatis P, Waser B, Reubi JC, et al. Potent bombesin-like peptides for GRP-receptor targeting of tumors with ^{99m}Tc: a preclinical study. J Med Chem 2005;48:100–10.
17. Cuttitta F, Carney DN, Mulshine J, Moody TW, Fedorko J, Fischler A, et al. Bombesin-like peptides can function as autocrine growth factors in human small-cell lung cancer. Nature 1985;316:823–6.
18. Jensen RT, Coy DH. Progress in the development of potent bombesin receptor antagonists. Trends Pharmacol Sci 1991;12:13–9.
19. Llinares M, Devin C, Chaloin O, Azay J, Noel-Artis AM, Bernad N, et al. Syntheses and biological activities of potent bombesin receptor antagonists. J Pept Res 1999;53:275–83.
20. Cescato R, Maina T, Nock B, Nikolopoulou A, Charalambidis D, Piccand V, et al. Bombesin receptor antagonists may be preferable to agonists for tumor targeting. J Nucl Med 2008;49:318–26.
21. Abd-Elgaliel WR, Gallazzi F, Garrison JC, Rold TL, Sieckman GL, Figueroa SD, et al. Design, synthesis, and biological evaluation of an antagonist-bombesin analogue as targeting vector. Bioconjug Chem 2008;19:2040–8.
22. Mansi R, Wang X, Forrer F, Kneifel S, Tamma ML, Waser B, et al. Evaluation of a 1,4,7,10-tetraazacyclododecane-1,4,7,10-tetraacetic acid-conjugated bombesin-based radioantagonist for the labeling with single-photon emission computed tomography, positron emission tomography, and therapeutic radionuclides. Clin Cancer Res 2009;15:5240–9.
23. Heppeler A, Froidevaux S, Mäcke H, Jermann E, Béhé M, Powell P, et al. Radiometal-labelled macrocyclic chelator-derivatised somatostatin analogue with superb tumour-targeting properties and potential

for receptor-mediated internal radiotherapy. Chem Eur J 1999;5:1974–81.
24. Azay J, Nagain C, Llinares M, Devin C, Fehrentz JA, Bernad N, et al. Comparative study of in vitro and in vivo activities of bombesin pseudopeptide analogs modified on the C-terminal dipeptide fragment. Peptides 1998;19:57–63.
25. Coy DH, Mungan Z, Rossowski WJ, Cheng BL, Lin JT, Mrozinski JE Jr, et al. Development of a potent bombesin receptor antagonist with prolonged in vivo inhibitory activity on bombesin-stimulated amylase and protein release in the rat. Peptides 1992;13:775–81.
26. Atherton E, Sheppard R. Fluorenylmethoxycarbonyl-polyamide solid phase peptide synthesis. General principles and development. Oxford: Oxford Information Press; 1989.
27. Velikyan I, Beyer GJ, Langstrom B. Microwave-supported preparation of (68)Ga bioconjugates with high specific radioactivity. Bioconjug Chem 2004;15:554–60.
28. Reubi JC, Wenger S, Schmuckli-Maurer J, Schaer JC, Gugger M. Bombesin receptor subtypes in human cancers: detection with the universal radioligand (125)I-[D-TYR(6), beta-ALA(11), PHE(13), NLE(14)] bombesin(6-14). Clin Cancer Res 2002;8:1139–46.
29. Vigna SR, Mantyh CR, Giraud AS, Soll AH, Walsh JH, Mantyh PW. Localization of specific binding sites for bombesin in the canine gastrointestinal tract. Gastroenterology 1987;93:1287–95.
30. Fleischmann A, Laderach U, Friess H, Buechler MW, Reubi JC. Bombesin receptors in distinct tissue compartments of human pancreatic diseases. Lab Invest 2000;80:1807–17.
31. Forrer F, Valkema R, Bernard B, Schramm NU, Hoppin JW, Rolleman E, et al. In vivo radionuclide uptake quantification using a multi-pinhole SPECT system to predict renal function in small animals. Eur J Nucl Med Mol Imaging 2006;33:1214–7.
32. Rogers BE, Bigott HM, McCarthy DW, Della Manna D, Kim J, Sharp TL, et al. MicroPET imaging of a gastrin-releasing peptide receptor-positive tumor in a mouse model of human prostate cancer using a ^{64}Cu-labeled bombesin analogue. Bioconjug Chem 2003;14:756–63.
33. Maddalena ME, Fox J, Chen J, Feng W, Cagnolini A, Linder KE, et al. ^{177}Lu-AMBA biodistribution, radiotherapeutic efficacy, imaging, and autoradiography in prostate cancer models with low GRP-R expression. J Nucl Med 2009;50:2017–24.
34. Aprikian AG, Han K, Chevalier S, Bazinet M, Viallet J. Bombesin specifically induces intracellular calcium mobilization via gastrin-releasing peptide receptors in human prostate cancer cells. J Mol Endocrinol 1996;16:297–306.
35. Wadas TJ, Eiblmaier M, Zheleznyak A, Sherman CD, Ferdani R, Liang K, et al. Preparation and biological evaluation of ^{64}Cu-CB-TE2A-sst2-ANT, a somatostatin antagonist for PET imaging of somatostatin receptor-positive tumors. J Nucl Med 2008;49:1819–27.
36. Maecke HR, Hofmann M, Haberkorn U. (68)Ga-labeled peptides in tumor imaging. J Nucl Med 2005;46 Suppl 1:172S–8S.
37. Sato N, Gleave ME, Bruchovsky N, Rennie PS, Beraldi E, Sullivan LD. A metastatic and androgen-sensitive human prostate cancer model using intraprostatic inoculation of LNCaP cells in SCID mice. Cancer Res 1997;57:1584–9.
38. Jantscheff P, Ziroli V, Esser N, Graeser R, Kluth J, Sukolinskaya A, et al. Anti-metastatic effects of liposomal gemcitabine in a human orthotopic LNCaP prostate cancer xenograft model. Clin Exp Metastasis 2009;26:981–92.
39. Vauquelin G, Van Liefde I, Birzbier BB, Vanderheyden PM. New insights in insurmountable antagonism. Fundam Clin Pharmacol 2002;16:263–72.